# Damages Influence on Dynamic Behaviour of Composite Structures Reinforced with Continuous Fibers

**GILBERT-RAINER GILLICH[1], ZENO-IOSIF PRAISACH[1], IONICA NEGRU[1]**
[1]"Eftimie Murgu" University of Reşiţa, Department of Mechanical Engineering, 1-4 P-ta Traian Vuia, 320085, Resita, Romania

*The paper presents an algorithm to assess damages in composite structures, based on how natural frequencies of weak-axes bending vibration modes change due to damage. The authors have contrived a correlation between the strain energy stored in a segment of a beam-like structure and the frequency change for that mode if damage occurs on that segment. Finding that the dynamic behavior of composite structures can be best modeled using the share model, which consider the bending moment together with lateral displacement and share deformation, we worked out a relation which gives the frequency shift of all bending modes, involving one coefficient depending on the support type. To evaluate damages, we determine analytically the relative frequency shift as ratio between the frequency change and the natural frequency of the undamaged beam, for the more vibration modes, considering a large number of damage scenarios. Comparing these results with that obtained by measurements on the real structure, it is possible to detect and locate damages with high precision. The method was validated by numerous experiments.*

*Keywords: composite materials, fiber reinforcement, damage detection, natural frequency*

Composites as manufactured materials consist from two or more constituents with quite different physical and/or chemical properties, which can be identified separately and distinctively within the finished structure. Unlike to natural materials which have predefined properties, composites are elaborated to fulfill predefined needs, permitting a new approach in structural design [1]. Compared with metals, composites are less heavy and can attain higher strength properties, which impose them in numerous engineering applications.

Fiber-reinforced composite materials can be divided into two categories, continuous fiber-reinforced composites and short fiber-reinforced composites respectively. Continuous reinforced composites can have uni-, bi- or multi-directional fibers as well as woven fibers and may often constitute a layered or laminated structure. On the other hand, short fiber-reinforced composites contain discontinuous, parallel or randomly oriented fibers.

Among continuous fiber-reinforced composites we can nominate fiberglass or glass-fiber reinforced plastic (GFRP), carbon-fiber reinforced plastic (CFRP) and Aramid-fibre reinforced plastic (AFRP). Table 1 presents typical combinations of fiber and matrix materials of the above mentioned composites [2 - 4].

Properties of composite reinforcing fibers have strength and stiffness far above those of traditional bulk materials, as illustrated in table 2, diluted in combination with the matrix materials to some degree, but thus very high specific properties are available from these materials [5].

The fibers can be placed in different layers and oriented within the material in various directions to obtain desired properties for the composite. Such materials, known as

| Reinforcing Material | Usual Matrix Materials |
|---|---|
| Glass Fiber<br>▪ E-Glass<br>▪ S-Glass | Epoxy (EP)<br>Polyester<br>Vinylester (VE)<br>Polyamide (PA or Nylon)<br>Polycarbonate (PC)<br>Polypropylene (PP)<br>Polybutylene terephthalate (PBT)<br>Polyoxymethylene (POM or Acetal) |
| Carbon Fiber<br>▪ HS graphite<br>▪ HM graphite | Epoxy (most often)<br>Polyester<br>Vinylester (VE) |
| Aramid Fiber | Polyamide (PA or Nylon) |

**Table 1**
TYPICAL FIBER-MATRIX COMBINATIONS

| Material | Young's modulus $E$ (GPa) | Breaking stress $\sigma_b$ (GPa) | Breaking strain $\varepsilon_b$ (%) | Density (kg/m$^3$) |
|---|---|---|---|---|
| E-glass | 72.4 | 2.4 | 2.6 | 2540 |
| S-glass | 85.5 | 4.5 | 2.0 | 2490 |
| HS graphite | 253 | 4.5 | 1.1 | 1800 |
| HM graphite | 520 | 2.4 | 0.6 | 1850 |
| Aramid | 124 | 3.6 | 2.3 | 1450 |

**Table 2**
PHYSICAL AND MECHANICAL PROPERTIES OF FIBERS

* *email: gr.gillich@uem.ro, zpraisach@yahoo.com, i.negru@uem.ro*
*Tel. 0730583049*

anisotropic, have different properties in different directions; the control of the anisotropy is an important means of optimizing the material for specific applications [4, 6]. Consequently, the physical properties of these materials, like stiffness, will often depend upon the orientation of the applied forces and/or moments in respect to the fiber orientation. Though, the final properties of the composite depend also on the fiber density (specific number of fibers per cross-section area).

Numerous attempts were made to model composite materials [1, 7, 8] in order to facilitate proper design of structures involving composites, especially oriented in design of new finite elements. The developed models can be successful involved in static problems, but do not offer a relation between a possible damage and dynamic characteristics of the composite structure like natural frequencies or mode shapes and their derivatives. These futures are used in global evaluation of structure integrity, various nondestructive techniques being available for specific applications [9]. A comprehensive review of vibration-based damage identification methods can be found in [10], where are also revealed the limitations and weaknesses of these methods. To overcome these problems the authors of this paper have performed an in-deep research of the phenomena occurring by the appearance of damages in beams [11] and established a relation available for all types of beam support and geometry. It permits, by implying a method also developed by the authors, an exact location and evaluation of damage in isotropic materials [12]. This paper presents an extension the damage detection method on anisotropic materials like layered or sandwich composites.

## Vibration-based damage detection method adapted for composites

Previous work done on this field by the authors, [9, 11, 12], lead to the development of a method proper to detect, locate and evaluate damage severity in isotropic Euler-Bernoulli beams. In order to extend the availability of the method on composites, analytical and numerical investigations where done as well as experiments. In our investigations we considered a cantilever steel beam with length $L$ = 1000 mm; width $B$ = 50 mm and height $H$ = 5 mm. Consequently, for the undamaged state the beam has the cross-section $A = 250 \cdot 10^{-6}$ m$^2$ and the moment of inertia $I = 520.833 \cdot 10^{-12}$ m$^4$. The material parameters of the specimens are: mass density $\rho$ = 7850 kg/m$^3$; Young's modulus $E = 2.0 \cdot 10^{11}$ N/m$^2$, tensile strength $\sigma_a$ = 460 MPa, and Poisson's ratio $\mu$ = 0.3. Afterwards we considered a composite beam, realized by gluing four groups of layers (laminae) with different fiber orientations, like shown in figure 1. The outer laminae groups contain fibers oriented parallel to the longitudinal axes of the beam, having the orientation angle $\theta_{1,4} = 0°$, while the inner laminae groups contain fibers with an orientation angle $\theta_2 = 45°$ and $\theta_3 = -45°$ respectively.

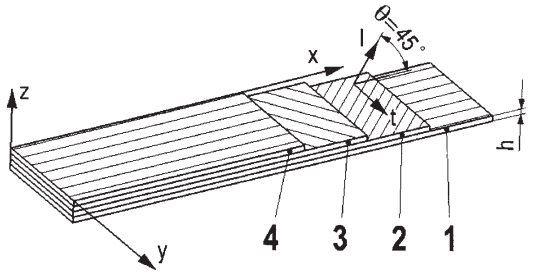


Fig.1. Layered fiber reinforced composite

The composite cantilever beam has also the length $L$ = 1000 mm, width $B$ = 50 mm, each group of laminae having the height $h$ = 1.25 mm. For a better comparison, but without significantly affecting the results, the outer lamine groups maintain the mechanical characteristics of the steel, whereas the inner laminae groups due symmetry have the same physical and mechanical characteristics, namely: density 960 kg/m$^3$, Young's modulus $E$ = 1100 N/m$^2$, tensile strength $\sigma_a$ = 33 MPa. This model also fit well the case of sandwich panels with steel layers framing a foam layer.

The analytic study starts with the well-known equations of motion for a cantilever beam, using the so-called share model, where bending and share are considered:

$$\frac{\partial^4 w(x,t)}{\partial x^4} - \frac{\rho}{kG}\frac{\partial^4 w(x,t)}{\partial x^2 t^2} + \rho A \frac{\partial^2 w(x,t)}{\partial t^2} = 0$$

$$\frac{\partial^4 \alpha(x,t)}{\partial x^4} - \frac{\rho}{kG}\frac{\partial^4 \alpha(x,t)}{\partial x^2 t^2} + \rho A \frac{\partial^2 \alpha(x,t)}{\partial t^2} = 0 \quad (1)$$

Here $w$ is the transverse displacement of the beam, $\alpha$ is the angle of rotation due to bending, $x$ the distance from the fixed end, $t$ the time, $G$ the shear modulus and $k$ a shape factor depending on the cross-section's shape. For a rectangle

$$k = \frac{10(1+\mu)}{12+11\mu} \quad (2)$$

Neglecting share the Euler-Bernoulli model results, whose equation of motion for a cantilever beam is given by relation:

$$\frac{\partial^4 w}{\partial x^4} + \frac{\rho A}{EI} \cdot \frac{\partial^2 w}{\partial t^2} = 0 \quad (3)$$

Damping has insignificant influence upon natural frequencies in both cases and therefore it is neglected.

The values of natural frequencies for the share model are obtained by solving equation (1). For $i$ vibration modes one obtain:

$$f_{SHn} = \frac{\sqrt{a_n - b_n}}{2\pi}\sqrt{\frac{kE}{2(1+\mu)\rho L^4}} \quad (4)$$

where $a_n$ and $b_n$ result from the characteristic equation (5) of the shear cantilever beam

$$\left(b^2 - a^2\right)ab \sin a \sinh b + \left(b^4 + a^4\right)\cos a \cosh b + 2a^2 b^2 = 0 \quad (5)$$

and $a$ and $b$ are in following relation

$$b = a\sqrt{\frac{1}{\gamma^2 i^2 a^2 + 1}} \quad (6)$$

With $\gamma^2$ we denoted $\sqrt{2(1+\mu)/k}$ and $i$ is the radius of gyration $\sqrt{i} = 1/A$

Now it is possible to write the mode shape as:

$$W_n(x) = \frac{b_n^2}{a_n}\Omega\left(-\cos a_n \frac{x}{L} + \cosh b_n \frac{x}{L}\right) + \sin a_n \frac{x}{L} - \frac{b_n^3}{a_n^3}\sinh b_n \frac{x}{L} \quad (7)$$

and the rotation due bending as:

$$\Psi_n(x) = \Omega\left(\frac{b_n^4}{a_n^4}\sin a_n \frac{x}{L} + a_n b_n \sinh b_n \frac{x}{L}\right) + \frac{b_n^2}{a_n}\cos a_n \frac{x}{L} - \frac{b_n^2}{a_n}\cosh b_n \frac{x}{L} \quad (8)$$

where we denoted $\Omega = \frac{a_n \sin a_n + b_n \sinh b_n}{b_n^2 \cos a_n + a_n^2 \cosh b_n}$

For the Euler-Bernoulli model the values of natural frequencies are obtained by solving equation (3); for *n* vibration modes one obtains:

$$f_{E-Bn} = \frac{\lambda_n^2}{2\pi}\sqrt{\frac{EI}{\rho A L^4}} \quad (9)$$

where $\lambda_n$ result from the characteristic equation (8) of the Euler-Bernoulli cantilever beam

$$1 + \cos\lambda \cdot \cosh\lambda = 0 \quad (10)$$

It is obvious that for a given beam, with constant rigidity *EI*, the ratio between natural frequencies $f_n$ and $f_{n+1}$ are given by the constants $a_n$, and $b_n$ or $\lambda_n$ respectively. Comparing these ratios with those of the values obtained on the real beam we can define its dynamic behavior. Table 3 presents the ratios for the Euler-Bernoulli model, shear model and that resulted by FEM analysis, where the first natural frequencies for the analytic cases were normalized to fit that of the FEM analysis; however, differences are less than 1.5%.

Dividing the ratios obtained using the FEM to those of the Euler-Bernoulli model and Share model respectively we can find out the manner how the real beam behaves. Figure 2 presents these results in a graphical way, suggesting the similar behavior of the beam to that of the Share model.

The facts presented above lead us to the conclusion that the damage detection method developed by the authors for the isotropic case [12] is less appropriate for composite beams, as long as it base on mode shape curvature due bending alone. Differences between the behavior for the two cases are illustrated in figures 3 and 4, by plots of the mode shape and natural frequency changes respectively, where the continuous line is assigned to the Share model, while the dashed line represents the Euler-Bernoulli model.

One can observe that the inflection points and extrema points in figure 3 are lightly translated to the fixed end, so new patterns have to be designed; the effect is even higher as shorter the beam and higher the frequency mode. Similar conclusions can be found in [13]. For this reason, we propose to substitute the mode shape curvature in the Gillich-Praisach relation for the Euler-Bernoulli case, presented in [12], with the normalized potential energy, resulting a general available relation for all beam types and geometries. The relation, revealing frequency changes $\Delta f_n(x)$ at any location *x* along the beam and for any damage depth $\delta$, as difference between the frequency of the undamaged beam $f_{n\_U}$ and that of the damaged beam $f_{n\_U}(x)$, becomes in this case:

$$\Delta f_n(x) = f_{n\_U} - f_{n\_D}(x) =$$
$$= f_{n\_U} \cdot c_\alpha \cdot c_s \frac{H}{L} \cdot \left(\frac{\delta}{H-\delta}\right)^{\frac{3}{2}} c_b \frac{\overline{W} \cdot \overline{L}^2}{6} \cdot \overline{U}(x) \quad (11)$$

The right expression of equation (11) contains information extracted from the undamaged beam, excepting the damage location *x* and depth $\delta$. It has to be mentioned that this equation is valid for all vibration modes and support types as it is, for any beam model, without other alterations being necessary.

Equation (11) reveals the influence of each factor on frequency changes. Temperature influence is considered by $c_\alpha$ coefficient; for ambient temperature 22° this takes the unit value. The influence of beam geometrical dimensions is provided by the height *H* and length *L*, weighted by shape coefficient $c_s$. The influence of the cross-section reduction is represented by the bracket term; as expected, the enlargement of damage depth $\delta$ amplifies the frequency shift. The boundary conditions (beam support type) are represented in the relation by the sum of areas of

| Mode n | Analytic E-B [Hz] | Freq. ratio E-B | Analytic shear [Hz] | Freq. ratio Shear | FEM [Hz] | Freq ratio FEM |
|---|---|---|---|---|---|---|
| 1 | 5.148 | - | 5.148 | - | 5.148 | - |
| 2 | 32.260 | 6.267 | 31.74806 | 6.167 | 31.574 | 6.134 |
| 3 | 90.329 | 2.800 | 87.37779 | 2.752 | 86.929 | 2.753 |
| 4 | 177.009 | 1.960 | 167.2678 | 1.914 | 166.430 | 1.915 |
| 5 | 292.609 | 1.653 | 269.0946 | 1.608 | 267.396 | 1.607 |
| 6 | 437.107 | 1.494 | 389.8079 | 1.448 | 386.579 | 1.446 |
| 7 | 610.505 | 1.397 | 526.1991 | 1.349 | 520.847 | 1.347 |
| 8 | 812.803 | 1.331 | 675.0105 | 1.282 | 667.366 | 1.281 |
| 9 | 1044.000 | 1.284 | 833.4776 | 1.234 | 823.700 | 1.234 |
| 10 | 1304.096 | 1.249 | 999.6379 | 1.199 | 987.842 | 1.199 |

**Table 3**
NATURAL FREQUENCIES OF THE COMPOSITE CANTILEVER BEAM AND THE FREQUENCY RATIOS

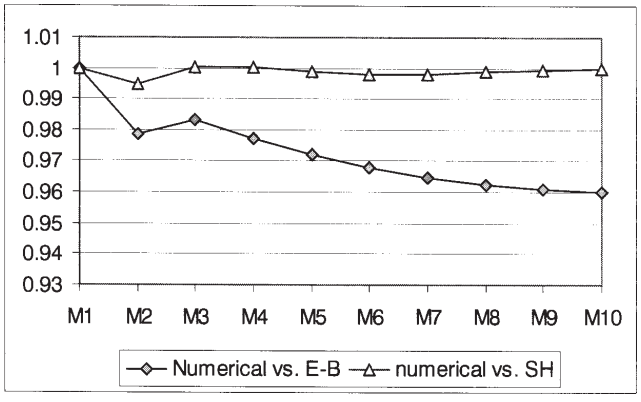


Fig.2. Comparison between the behavior of the composite beam and the Euler-Bernoulli and Share beam respectively

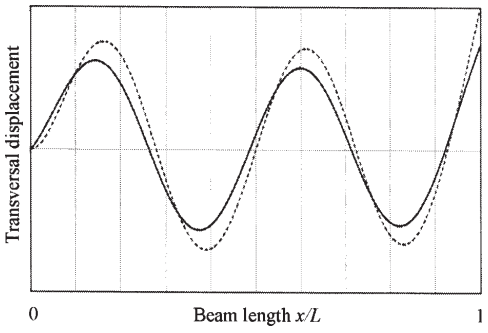


Fig.3. Typical mode shape for a beam modeled using the Shear model — and Euler-Bernoulli model - - - respectively

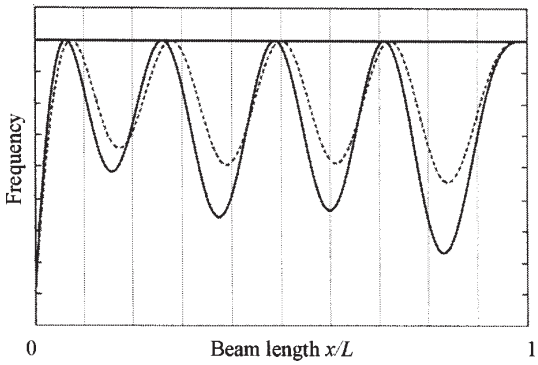


Fig.4. Natural frequency changes due damage for a beam modeled using the Shear model — and Euler-Bernoulli model - - - respectively

bending moments acting on the beam, calculated for normalized weight W and length L, weighted with $c_b$ coefficient placed before the third fraction. For the cantilever beam $c_b$ = 1 as well as for the simple supported and the double clamped one. For the beam clamped at one end and pinned at the other it is 0.875.

Damage location influence is introduced by the normalized potential energy at the location $x$ along the beam, being determined using relation:

$$\overline{U}(x)=\frac{[\Psi'(x)]^2+kGA[W'(x)-\Psi(x)]^2}{max\left|[\Psi'(x)]^2+kGA[W'(x)-\Psi(x)]^2\right|} \qquad (12)$$

Obvious, at the location $x$ for which $\overline{U}n(x) = 1$, highest frequency shift is achieved for the corresponding vibration mode. In this case, a global coefficient $c$ can be defined as:

$$c=c_\alpha\cdot c_s\frac{H}{L}\cdot\left(\frac{\delta}{H-\delta}\right)^{\frac{3}{2}}c_b\frac{\overline{W}\cdot\overline{L}^2}{6} \qquad (13)$$

which is constant for a given beam with certain damage, irrespective to vibration mode number $n$. The normalized potential energy is the only factor controlling the influence of damage location; in the meantime the $c$ coefficient from equation (11) indicates the influence of damage depth. In literature, for isotropic materials, the relation between damage depth and frequency change is considered quasi-exponential, [14, 15]. For layered beams, this relation is perturbed by the differences of mechanical properties between laminae or groups of laminae. Simulations made by means of the FEM for the two specimens described in the beginning of the section, for the undamaged case and 32 damaged cases (eight levels of depth and four locations of damage considered one by one) for each beam, permitted the calculus of the relative frequency shifts $\Delta f_n^*(x)$ for ten vibration modes one, as the frequency shift $\Delta f_n(x)$ normalized by the frequency of the undamaged beam $f_{n\_U}$ for a given mode $n$.

To illustrate the differences between the behavior of damaged steel and composite beams respectively, we consider a transversal open damaged for both beams, having a width of 2 mm and a depth δ varying between 8 and 67%, placed at distance $x$ from the clamped end, like it is presented in figure 5.

Results of simulations made using the FEM, presented in figure 6 for the vibration mode one, reveal that for the steel beam the relative frequency shift increase exponentially with damage depth (as expected), while for the composite beam the increase of the relative frequency

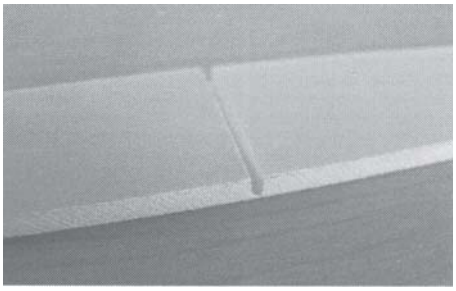

Fig.5. Damage induced in the composite beam, for a depth of 67%

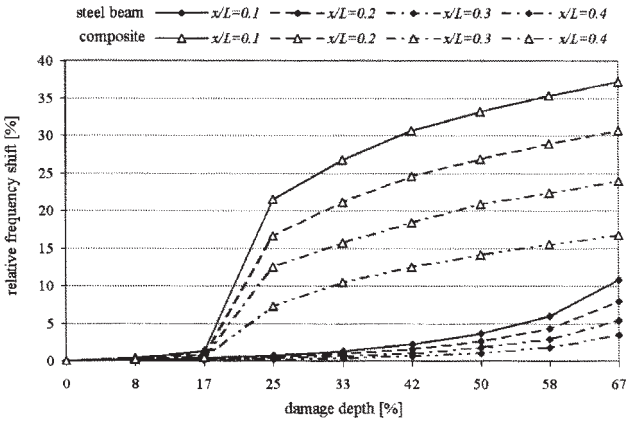


Fig.6. Relative frequency shift for the steel and the composite beam, for various locations and levels of depth

shift present a step when its depth is nearby the height of the outer laminae.

It is obvious that for a composite made by a larger number of layers, the evolution of the relative frequency shift is stepwise; the higher the number of different layers, the smaller the step. On the other hand, significant differences between the layer characteristics (especially density) lead to significant values of the relative frequency shift. One also observe that the relative frequency shift take higher values for the composite beam, even for reduces values of damage; consequently, damage detection is more facile for composite beams. However, this effect is also amplified by significant density differences between the layers.

**Experimental results and validation of the method**

To prove the method availability a series of experimental tests where performed on a composite beam. The chosen beam support type was fixed-free, realized mounting it in a rigid support. The measurement system used for the vibration signal acquisition, presented in figure 6, is composed by a Toshiba laptop, a NI cDAQ-9181 single slot chassis with Ethernet connection, a NI 9234 four-channel dynamic signal acquisition module and a Kistler 8772A10M10 piezoelectric accelerometer. This system permits transmission of data to larger distances, useful when monitored structures are distributed on a larger field. As programming environment LabVIEW was used to develop the virtual instrument which acquire the time history of acceleration and realize the spectral analysis. It has to be mentioned that this virtual instrument is designed to find the natural frequencies with high accuracy, though early damage detection implies observation of small frequency changes.

To find out the weak-axes bending natural frequencies for the first ten vibration modes we measured the accelerations on transversal direction. The accelerometer was placed near the free end of the beam, figure 7, in a

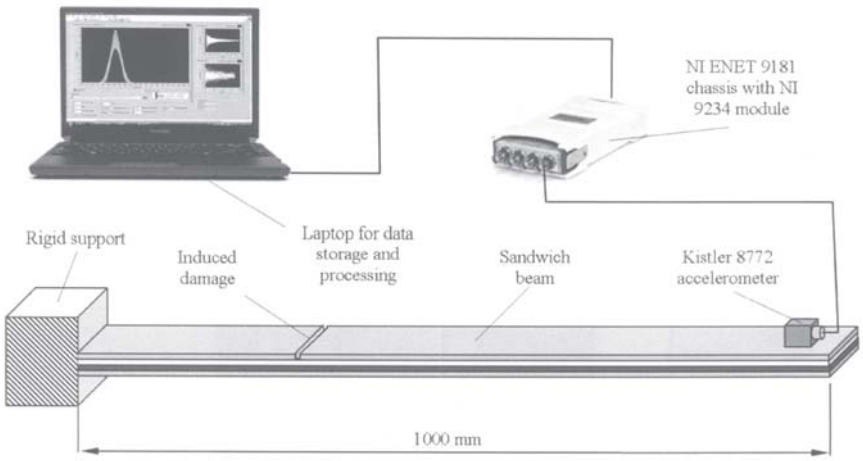


Fig.7. Experimental stand

| Mode | Natural frequency $f_n$ | | Relative frequency shift $\Delta f_n^*$ | |
|---|---|---|---|---|
| | Undamaged | Damaged | Percentage | Normalized |
| | [Hz] | [Hz] | [%] | [-] |
| 1 | 5.14 | 4.52 | 12.06226 | 1 |
| 2 | 31.55 | 30.63 | 2.916006 | 0.241746 |
| 3 | 87.13 | 78.21 | 10.23758 | 0.848728 |
| 4 | 166.15 | 161.82 | 2.606079 | 0.216052 |
| 5 | 267.87 | 263.74 | 1.541793 | 0.12782 |
| 6 | 387.71 | 359.45 | 7.288953 | 0.604278 |
| 7 | 522.43 | 506.94 | 2.964991 | 0.245807 |
| 8 | 669.57 | 668.79 | 0.116493 | 0.009658 |
| 9 | 826.93 | 789.04 | 4.582008 | 0.379863 |
| 10 | 991.38 | 959.85 | 3.180415 | 0.263667 |

**Table 4**
MEASURED NATURAL FREQUENCIES AND CORRESPONDING SHIFTS FOR THE ANALYZED BEAM

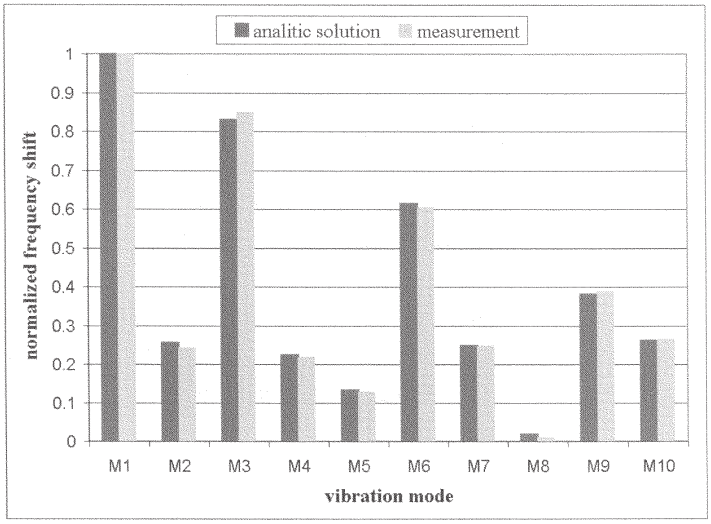


Fig.8. Pattern recognition for a induced damage at 300 mm from the fixed end

location assuring reasonable displacement, determined from the mode shapes. A transversal force was applied on the beam to bring the mechanical system out of its equilibrium position; suppressing that force, the beam started to vibrate. We recorded the acceleration values for the undamaged beam and stored them on the laptop; afterwards we determined the natural frequencies for the first ten bending vibration modes. The process was repeated until trustful frequency values were obtained. The results can be improved by replacing the accelerometer on certain points, where the maximum displacement for the corresponding mode is obtained. Afterwards, a damage on the beam was produced by a saw cut at around 300 mm from the fixed end with a certain depth (which will be determined subsequently) and new series of measurement realized. The obtained results are presented in table 4, both for undamaged and damaged case. It is obvious that for the damaged beam some frequencies present changes comparative to the undamaged case, while other frequencies maintain their values. This make possible to precisely identify the location of damage and afterwards its severity by using an algorithm developed by the authors [12].

Using the measured natural frequency values of the weak-axes bending vibrations for the undamaged and damaged case, one can calculate the relative frequency shift $\Delta f_n^*(x)$ in percents and normalized with the highest value of the series. The results are also presented in table 4. It is evident that whereas the relative frequency shift expressed in percents provide information about the location and depth of damage, the results expressed in dimensionless units provide information about the damage

location exclusively. For a precise location it is recommendable to compare first these last values with those obtained analytically for numerous damage locations; similarity between the series determined by measurements and patterns determined analytically define the damage location [12]. Figure 8 presents the patterns for a damage at 300 mm from the fixed end (left columns) and the series of values determined using the measured frequencies (right columns); one can observe the good fit between them. Therefore, damage location is reduced to a pattern recognition problem.

Knowing the location of the damage, respectively the value $x/L = 0.3$, we can evaluate the damage severity by finding the place on the corresponding curve in figure 5 on which the relative frequency shift takes the value 12%. Thus we estimate a cross-section reduction due damage of almost 25%. Dimensional measurement confirms a damage depth a little higher than 1 mm, representing a cross-section reduction of 20-22%.

## Conclusion

Researches performed by the authors, presented in this paper, have find out that composite beams follow a dynamic behavior best described by the share model. This imposes, for accurate damage detection and location, the use of new patterns based on the generalized relation given in equation (11). However, like by isotropic materials, on inflection points of the mode shape curvature no frequency changes occur, while on extreme points highest changes appear.

Damage depth lead to a stepwise evolution of frequency changes; the number of steps and their height are defined by the number of layers. The relative frequency shift depends especially on the difference between layers properties, bigger differences leading to bigger shifts in frequency. This makes damage detection and location in composite beams more facile comparative to steel beams, but estimation of damage severity more difficult.

As future work, the authors intend to extend their researches on plates and shells.

*Acknowledgements : The authors gratefully acknowledge the support of the Managing Authority for Sectoral Operational Programme for Human Resources Development (MASOPHRD), within the Romanian Ministry of Labour, Family and Equal Opportunities by co-financing the project "Excellence in research through postdoctoral programmes in priority domains of the knowledge-based society (EXCEL)" ID 62557.*

## References

1. ILIESCU, N., HADAR, A., PASTRAMA, S.D., Mat Plast., **46**, no. 1, 2009, p. 91
2. XIAOSONG HUANG, "Fabrication and Properties of Carbon Fibers", Materials, **2**, 2009, p. 2369
3. SPYRIDES, S.M.M., BASTIAN, F.L., "In vitro comparative study of the mechanical behavior of a composite matrix reinforced by two types of fibers (polyethylene and glass)", Mat. Sci. Eng. C – Mater., **24**, 2004, p. 671
4. CORUM, J. M., BATTISTE, R. L., LIU, K. C., RUGGLES, M. B., "Basic properties of reference crossply carbon-fiber composite", Report, February 2000, p. 21
5.GERSTLE, F.P., "Composites", Encyclopedia of Polymer Science and Engineering, Wiley, New York, 1991, p. 36
6. HADĂR, A., GHEORGHIU, H., BACIU, F., DINCA, A., TUDOR, D.I., "Modification of The Mechanical Behaviour of Fiber Reinforced Composite Materials under the Action of the Ad Type Bio-Phyto-Modulators", Bulletin UASVM, Horticulture, **67**, nr. 2, 2010, p. 505
7. CHEN, G.M., CHEN, J.F., TENG, J.G., "On the finite element modelling of RC beams shear-strengthened with FRP", Constr. Build. Mater., **32**, 2012, p. 13
8. CUNHA, V., BARROS, J., SENA-CRUZ, J., "A finite element model with discrete embedded elements for fibre reinforced composites", Comput.Struct., 94–95, 2012, p. 22
9. GILLICH, G-R., PRAISACH, Z-I., MOACA-ONCHIS, D., "About the Effectiveness of Damage Detection Methods Based on Vibration Measurements", Proceedings of the 3rd International Conference on Engineering Mechanics, Structures, Engineering Geology, Corfu Island, Greece, July 22-24, 2010
10. DOEBLING, S.W., FARRAR, C.R., PRIME, M.B., "A summary review of vibration based damage identification methods", Shock Vib. Dig., **30**, nr. 2, 1998, p. 91
11. PRAISACH, Z.I., MINDA, P.F., GILLICH, G.R., MINDA, A.A., "Relative Frequency Shift Curves Fitting Using FEM Modal Analyzes", 4th International Conference on Finite Differences - Finite Elements - Finite Volumes - Boundary Elements, Paris, 28-30 April, 2011
12.GILLICH, G.-R., PRAISACH, Z.-I., "Robust method to identify damages in beams based on frequency shift analysis", SPIE Smart Structures/NDE, 8348-47, San Diego, California, USA, 2012.
13. GAOMING DAI, WEIHONG ZHANG, "Cell size effects for vibration analysis and design of sandwich beams", Acta Mech. Sin., **25**, 2009, p. 353
14. FERNANDEZ-SADEZ, J., RUBIO L., NAVARRO, C., "Approximate Calculation of the Fundamental Frequency for Bending Vibrations of Cracked Beams", J. Sound Vib., **225**, nr. 2, 1999, p. 345
15. SINHA, J.K., FRISWELL, M.I., EDWARDS, S., "Simplified Models for the Location of Cracks in Beam Structures using Measured Vibration Data", J.Sound Vib., **251**, nr. 1, 2002, p. 13

Manuscript received: 25.02.2012